

Predictive Modeling of Li-Air Batteries Using Artificial Neural Network: A Comparative Study of Cathode Morphology

Aisha Jilani^{1,2}, Zahoor Ul Hussain Awan^{1*}, Syed Ali Ammar Taqvi^{2*}

¹ Department of Food Engineering, NED University of Engineering and Technology, 75270 Karachi, Pakistan

² Department of Chemical Engineering, NED University of Engineering and Technology, 75270 Karachi, Pakistan

* Corresponding authors, e-mail: zahoor@cloud.neduet.edu.pk, aliammar@cloud.neduet.edu.pk

Received: 26 November 2024, Accepted: 07 February 2025, Published online: 24 February 2025

Abstract

The artificial neural network (ANN) modeling is used to analyze the impact of two different cathode morphologies urchins (α -MnO₂) and flower (δ -MnO₂), on the charge/discharge voltage in lithium air batteries (LABs). Previous research has focused on ANN models for traditional lithium-ion batteries (LIBs) without accounting for varied cathode morphologies in LABs. This research presents an ANN modeling technique to predict the charge/discharge voltage LAB using manganese oxide as cathode materials with two distinct morphologies. For modeling Specific capacity use as the input variable, to perform a comprehensive analysis to validate charge/discharge voltages. This study explores multiple ANN configurations with varying neuron counts, identifying the optimal architecture (10 neurons in hidden layers) that balances prediction accuracy and efficiency. This systematic exploration provides insights into ANN tuning for LABs, which is a topic with limited coverage in existing literature. The ANN predicted results closely matched with the reported experimental work with the coefficient of determination $R^2 = 0.9998$ for almost all models. The models performance was assessed by various error metrics mean absolute deviation (MAD), root mean square error (RMSE) and average absolute relative error (AARE). This study provides empirical validation of the model's robustness. The study highlights the applicability of ANN in capturing complex LAB performance metrics, such as the non-linear behaviors due to morphological differences.

Keywords

lithium air battery, energy storage, artificial neural network

1 Introduction

Global warming is elevated due to the usage of excessive fossil fuels. The growing need for sustainable, eco-friendly energy sources is driven by the need to reduce dependence on fossil fuels, which contributes to pollution, resource depletion and rising costs. Transitioning to renewable energy and minimizing high-pollution industries are essential for mitigating environmental and economic risks [1]. Additionally, these conventional fuels risk depleting natural resources [1]. A noteworthy development has been the exploration and utilization of various renewable energy sources, attributes to the efforts of researchers worldwide [2]. Lithium air batteries (LABs) are promising energy storage technology, with a theoretical energy density of 3500 Wh/kg, significantly higher than 400 Wh/kg of lithium-ion battery (LIB). This makes them strong candidate for electric vehicles (EVs) and hybrid electric vehicles (HEVs), providing longer operational performance and potentially replacing petroleum

as a fuel source. LABs are classified into four types based on their electrolytes: aprotic, aqueous, hybrid and solid-state electrolyte LABs. Aqueous LABs are being widely studied worldwide. Despite their potential, LABs face significant challenges, including low operating voltages, capacity degradation, short cycle life slow oxygen evolution/reduction kinetics and increasing overpotential. Surpassing the LIBs which is greater than LIBs energy density i.e., 400 Wh/kg. LAB is utilizing the lithium, hold an energy density of 11682 Wh/kg and capacity of 3863 Ah/kg and at 3.0 V. This endures to designate an energy efficiency of approximately 1000 Wh/kg.

In a LAB, the anode lithium oxidation response happens much speedier than the cathode oxygen decrease response (OER), and the cathode response over potential is altogether higher than the anode response [3]. Therefore leading the overall rate of battery charge/discharge [4, 5]. Because of this, scientists have focused much

more on the cathode in LABs than on the anode, resulting in many research and development plans worldwide. Even though there haven't been any big discoveries lately, a lot of progress has still been achieved. The main problem that stops making practical LAB applications is that air cathodes aren't very efficient right now [6]. To enhance the performance of cathode material, many structures, materials and synthesis processes have been investigating for cathode in the last decade [5, 7]. Cathodes with higher capacity are significant for electronic market consumer. Improved security, enhanced rate capability, lower cost, are few main conditions for applications such as HEVs [4]. Manganese oxides as cathodes have gained specific consideration because of notable advantages they have, such as abundance, less cost, high alkaline activity, high specific capacity and nontoxic in nature.

MnO₂ exists in different morphological shapes like nano tubes, nano sheets, flowers, urchins, and nano spheres [8] Extensive studies are conducted to investigate manganese oxides as an active cathode material with various morphologies in LABs. [7, 9, 10]. Safety and life time of battery estimation and modeling techniques are important in order to progress the performance, Allowing the battery to age, will more likely increase the expenses, shorten the life and also compromise the battery security. It is very significant to accurately estimate the various battery parameters to predict the life span of batteries. Development in soft computing and computer science has led to improved attention in the progress for predictive modeling for expensive and time-consuming investigations [11]. Researchers face challenges in collecting accurate data for developing new technologies. Artificial intelligence (AI) particularly machine learning (ML) and artificial neural network (ANN), offers a promising approach to predicting key LAB performance metrics like voltage, capacity and failure points. ANN excel at pattern recognition, handling noisy data and adapting to environmental changes with applications in LABs, image recognition, automation and nonlinear programming. However, ANN development is complex, requiring careful design of network structure, weight initialization and thresholds, along with significant data and computational resources for training. Support vector machine (SVM), random forest (RF), gradient boosting machine (GBM), K-nearest neighbor (KNN) are few other ML modelling techniques. Each model has unique strengths and limitations. ANN are generally the favored choice for apprehending the non-linear performance and dynamic connections

in LABs. But, for smaller datasets or where interpretability is a concern, RF or SVM could be appreciated substitutes [12, 13]. With prolonged charge/discharge of battery, the performance of LAB will progressively reduce, as a result of which many safety concerns arise. ANN is supervised learning technique that was developed for modelling and simulating the learning capacities of biological cells and the human brain. Because of its capacity to comprehend complex and nonlinear phenomena, it is considered a noteworthy and dependable source that has attracted interest in the field of predictive modelling [14]. ANN excel at detecting nonlinear correlations in large datasets, but often require substantial training data to make correct predictions. ANN components are inspired by the biological nervous system. These components are arranged in node-connected linking layers. The input layer, hidden layer, and output layer are the three different categories of layers that form the working network to improve the capacity and capability of the network number of neurons and hidden layers must be chosen carefully. The networks and models are trained and modified to guide the inputs towards the desired target output ANN processed of iterating the weights till an optimal relation among the output and the targets is attained. There are many neural networks available for the modelling, like general regression neural networks (GRNN), feed-forward neural network (FFNN) [15], back propagation neural network (BPNN) [16], recurrent network (RN), radial basis function neural network (RBFNN) [17], long short-term memory networks (LSTM) [18], and probabilistic neural networks (PNN). Amongst all models, the FFNN are extensively employed for battery modeling areas. It consists of single layer and multi-layer perceptron and information is one directional. The generated signal by the input layer is transferred to the hidden layer. Where the activation function approaches the network's biases and weights using a learning model technique. The output created is referred to as the projected.

The Levenberg-Marquardt (LM) algorithm is efficient for training ANNs in LAB modelling, minimizing error by adjusting weights and biases. Metrics like root mean square error (RMSE), average absolute relative error (AARE), and mean absolute deviation (MAD) helps to optimize hyperparameters and prevent overfitting ensuring accurate predictions. A systemic approach to hyperparameter is employed, where number of neurons in hidden layer and other model parameters were tested to identify the optimal model configuration. Battery parameters such

as battery capacity, battery cycle life, charge/discharge voltage, state of charge (SOC), state of health (SOH), and remaining useful life (RUL) are used for battery testing and to analyze battery performance [19]. The charge/discharge cycle is crucial for battery performance and design optimization. While ML including ANN has been widely applied to other batteries like LIBs, its application to LABs remains unexplored due to unique LAB nonlinear behavior and electrochemical challenges. This study addresses this gap by developing an ANN model specifically for LABs, laying the groundwork for future research and expanding ML role in advanced battery technologies.

Continuous research into enhancing these cycles is dynamic for the evolution of battery technology, predominantly for applications in EVs and renewable energy storage devices. Therefore, the scope of this research is the development of an ANN model for the prediction of LAB charge/discharge voltage with published experimental data [20] experimental data. The two distinct models are developed with different numbers of neurons for both the cathode material morphologies. The performance of the ANN models was assessed using various error metrics, including RMSE, AARE, and MAD.

2 Methodology

2.1 Experimental setup

In this research, the most optimal crystalline structures of MnO_2 for the oxygen reduction reaction (ORR) are built on prior literature have been selected. Subsequently, conducted a comparative investigation of these structures as electro catalysts for the LAB cathode. The primary scope of the study is to assess and equate the catalytic properties of two different morphologies of MnO_2 nanoparticles. Through hydrothermal synthesis, we successfully prepared urchin ($\alpha\text{-MnO}_2$) and flower ($\delta\text{-MnO}_2$). The control of the hydrothermal reaction parameters facilitated the achievement of the distinct morphologies. The chemicals used for the synthesis of nanoparticles are listed in Table 1.

The urchin $\alpha\text{-MnO}_2$ nanoparticles were synthesized by adding $\text{MnSO}_4 \cdot \text{H}_2\text{O}$, $\text{K}_2\text{S}_2\text{O}_8$, and H_2SO_4 to deionized water. The solution was then shifted to a Teflon-lined autoclave and heated in a preheated oven at 110°C for 6 h. The brown precipitate was then centrifuged, washed, and then dried at 60°C for 8 h. The synthesis of flower $\delta\text{-MnO}_2$ involved transferring a solution of $\text{MnSO}_4 \cdot 3\text{H}_2\text{O}$ and KMnO_4 into a Teflon-lined autoclave, heating it in electric oven at 140°C for 2 h, and the brown precipitate was then centrifuged,

Table 1 List of chemicals used for synthesis [20]

S. No	Chemicals	Quantity
1	$\text{MnSO}_4 \cdot \text{H}_2\text{O}$	0.34 g
2	$\text{K}_2\text{S}_2\text{O}_8$	0.54 g
3	H_2SO_4	2 mL
4	$\text{MnSO}_4 \cdot 3\text{H}_2\text{O}$	0.2 g
5	KMnO_4	0.5 g

washed, and then dried at 40°C for 8 h. The nanoparticles were obtained from the synthesis process and are then used as cathode material for LAB. The battery has been tested for charge/discharge cycles limiting the maximum specific capacity of 800 mAh/g. Fig. 1 shows the battery voltage vs. specific capacity using urchin-shaped $\alpha\text{-MnO}_2$. Fig. 2 illustrates the same relationship for $\delta\text{-MnO}_2$. At 100% efficiency, a steady discharge/charge profile of 0.8 mAh was attained for almost 35 cycles with the urchin-shaped $\alpha\text{-MnO}_2$. There is a small voltage increase every ten cycles. A constant discharge/charge profile of 0.8 mAh was attained for 20 cycles

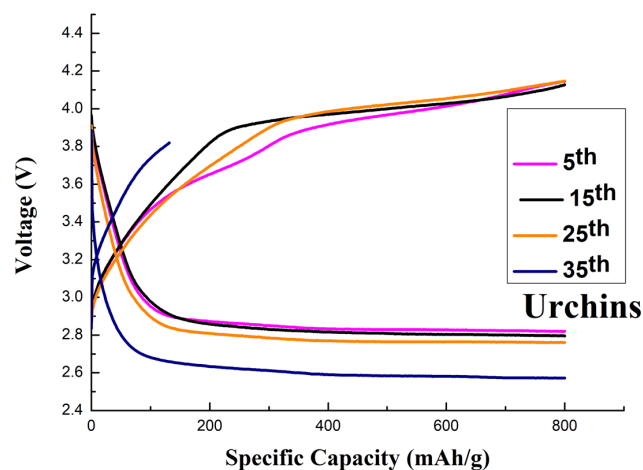


Fig. 1 Charge/discharge cycle for urchin morphology [20]

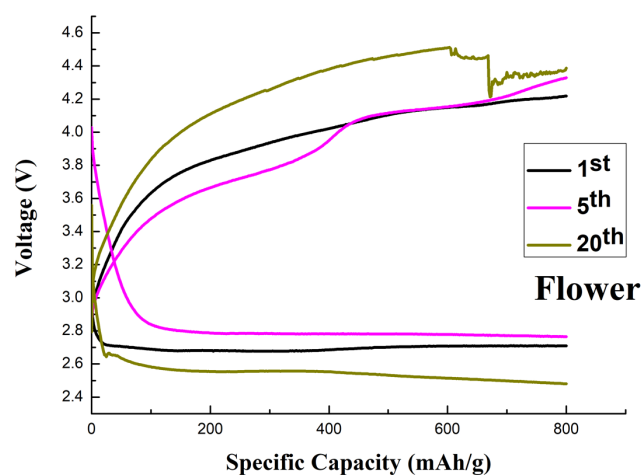


Fig. 2 Charge/discharge cycle for flower morphology [20]

with efficiency of 100% for δ -MnO₂. There was a noticeable rise in the overpotential of α -MnO₂ catalysts. The instability of δ -MnO₂ causes an increase in the overpotential after 20 cycles, worsening the charge curve and encouraging electrolyte disintegration. In order to improve the cycle performance the depth of charging and discharging is limited to 800 mAh/g [20]. The two battery parameters used in the research are battery voltage and specific capacity over the number of operating life cycles of the battery.

2.2 Development of ANN network approach

The ANN approach can predict or estimate parameters like SOC, SOH, voltage, operating cycles and current. Terminal voltage shows difference throughout discharge process interprets the nonlinear behavior of the LAB, and this difference greatly effects by the rate of discharge. The above-mentioned characteristics of LAB is designated by the charge/discharge curve (Figs. 1 and 2). In this study experimental data (specific capacity, voltage and number of cycles) is collected from [20] for two different MnO₂ morphologies i.e., urchins and flowers. ANN modeling is performed separately for charge and discharge cycle data for both urchins and flowers, afterward the charging and discharging ANN results are merged for the error functions calculations, for each morphology. The data size is huge, therefore a section of dataset is later used to find out the validity and robustness of the model. The performance of ANN is measured by MSE [21] given below:

$$\text{MSE} = \frac{1}{N} \sum_{i=1}^N (Y_{\text{ANN}} - Y_{\text{EXP}})^2 \quad (1)$$

Here ANN predicted output is referred as Y_{ANN} , the experimental data as Y_{EXP} and number of samples as N .

Software MATLAB [22] is used for the ANN modelling. First input and output parameters are selected. It was followed by data preprocessing and normalizing. Training: 70%, testing: 15% and validation: 15% is divided for the network. For this study the experimental data (i.e., inputs and outputs) are normalized with 0 and 1 value to upgrade the functionality of the network. Trial and error method is followed to select an optimal structure of ANN, applying the cross-validation outcomes everytime to see if the performance prediction can be improved. To validate the model cross-validation is one of the methods employed in this study. This technique splits the entire sample set into three parts: the training set, the validation set, and the testing set, usually in a fixed ratio. After the initial training session, the validation step enhances the training data more,

and finally, the testing set is used to check the capabilities when tested against a new set of data. Parameters used for the model are tabulated in Table 2.

The ANN model's performance is assessed by several error functions such as AARE, RMSE, MAD, and R^2 :

$$\text{RMSE} = \sqrt{\frac{\sum_{i=1}^n (Y_{\text{ANN}} - Y_{\text{EXP}})^2}{n}} \quad (2)$$

$$\text{AARE} = \left(\frac{\sum_{i=1}^n \left| \frac{Y_{\text{ANN}} - Y_{\text{EXP}}}{Y_{\text{ANN}}} \right|}{n} \right) \times 100 \quad (3)$$

$$\text{MAD} = \frac{1}{n} \sum_{i=1}^n |Y_{\text{ANN}} - Y_{\text{EXP}}| \quad (4)$$

$$R^2 = 1 - \frac{\sum_{i=1}^n (Y_{\text{ANN}} - Y_{\text{EXP}})^2}{\sum_{i=1}^n (Y_m - Y_{\text{obs}})^2} \quad (5)$$

3 Results and discussion

The input variable used for the neural network to predict the output voltage for charge/discharge cycles is the specific capacity. Five models of different numbers neurons (1, 5, 10, 15 and 20) are investigated for each charge and discharge data for both morphologies. The ANN predictive model is presented in the Fig. 3. The input/output layers are interrelated through elements referred as hidden neurons. The determination of number of neurons in the hidden layer is based on achieving minimum MSE. To obtain the optimal MSE for the trained model, various numbers of neurons is assessed, starting with least number. This procedure allows finding out the optimal value of number of neurons. In this scope of study, the ANN model was

Table 2 ANN model parameters

Particulars	Specifications
Algorithm	LM
Network	Feed forward neural network
Performance function	MSE
Division of data	Random
Data size	[1 × 800]
Input layers	1
Output layers	[35 × 800] for flowers [20 × 800] for urchins
Hidden neurons	Iterative
Learning cycles (Epochs)	1000

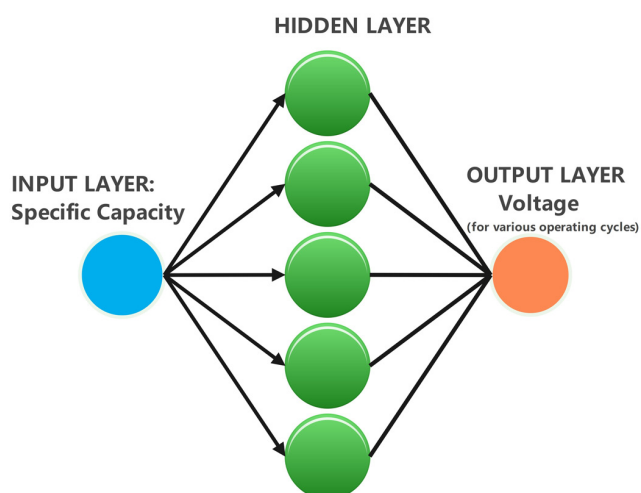


Fig. 3 ANN model to predict the charge/discharge voltage of LAB

undergoing training and tested for 1, 5, 10, 15 and 20 neurons. The network trained with 10 hidden neurons demonstrated to have the least value of MSE. It is noted that there are little discrepancies among experimental and modelled values. The error values illustrate that the predicted values are in decent agreement with experimental values.

The smaller the inaccuracy, the bigger is the R^2 value for the investigational and simulated results as shown in Table 3. Besides, the use of R^2 the developed ANNs performance for charge/discharge voltages was mathematically

calculated by various error functions types i.e., RMSE, AARE, and MAD, which were considered based on experimental and simulated results For urchine morphology the error metrics results are presented in Table 4 and for flower morphology results are presented in Table 5.

As tabulated in Table 4, for urchin morphology the errors (RMSE, MAD, and AARE) are relatively low in the first few cycles (5th and 10th) for the **1 neuron model**, which suggests that the model captures some level of the electrochemical behavior with minimal complexity. However, after the 25th cycle, there is an unexpected spike in the error metrics in the 35th cycle (RMSE = 0.4401, AARE = 44.97%). This sudden spike could indicate that the urchin morphology introduces additional complexity, such as clogging, degradation, or irregular lithium plating/stripping behavior that a simple 1 neuron model cannot capture over longer cycles. Despite performing well in the earlier cycles, the model breaks down when the battery undergoes more extensive cycling. After increasing neurons to **5** it showed much better stability across cycles, with RMSE remaining very low in early cycles (e.g., 5th cycle RMSE = 0.0086). Errors improve up until the 25th cycle (RMSE = 0.0061, AARE = 0.095%), indicating that this configuration handles the urchin morphology better by modeling the non-linear electrochemical processes more effectively. However, by the 35th cycle, the

Table 3 ANN structure for training, validation and testing data for urchins and flower morphologies

	Model	Neurons	MSE			R^2		
			Training	Validation	Testing	Training	Validation	Testing
Urchin charge	1	1	1.5198e-2	1.0287e-2	1.5501e-2	9.8105e-1	9.8824e-1	9.8135e-1
	2	5	2.0328e-4	2.7224e-4	8.8535e-5	9.9978e-1	9.9976e-1	9.9967e-1
	3	10	6.9166e-5	1.4391e-3	1.9156e-5	9.9990e-1	9.9831e-1	9.9998e-1
	4	15	2.1324e-3	1.3608e-3	1.5291e-3	9.9747e-1	9.9851e-1	9.9819e-1
	5	20	1.3350e-3	1.0217e-4	2.4085e-4	9.9847e-1	9.9988e-1	9.9971e-1
Urchin discharge	1	1	3.0130e-4	2.6702e-4	1.9850e-4	9.9581e-1	9.9624e-1	9.9712e-1
	2	5	5.1651e-5	4.4159e-5	2.7194e-5	9.9994e-1	9.9968e-1	9.9969e-1
	3	10	1.6909e-6	8.2766e-7	1.8693e-5	9.9990e-1	9.9997e-1	9.9971e-1
	4	15	1.4909e-6	1.7693e-5	8.2765e-7	9.9980e-1	9.9977e-1	9.9998e-1
	5	20	9.2801e-6	3.8239e-6	3.0171e-6	9.9972e-1	9.9996e-1	9.9996e-1
Flower charge	1	1	2.4357e-3	2.2376e-3	1.9930e-3	9.9037e-1	9.9242e-1	9.8866e-1
	2	5	1.7761e-4	1.4294e-4	1.9443e-4	9.9934e-1	9.9917e-1	9.9920e-1
	3	10	5.7951e-5	4.2996e-5	8.6624e-5	9.9979e-1	9.9984e-1	9.9963e-1
	4	15	4.7256e-5	3.0240e-5	2.8678e-5	9.9909e-1	9.9989e-1	9.9989e-1
	5	20	4.5943e-5	2.2478e-5	4.4486e-5	9.9980e-1	9.9989e-1	9.9983e-1
Flower discharge	1	1	1.4634e-3	3.2441e-4	2.0885e-4	9.7695e-1	9.9731e-1	9.9366e-1
	2	5	9.2041e-5	6.1606e-5	5.3953e-3	9.9864e-1	9.9908e-1	9.4170e-1
	3	10	1.1033e-3	3.2013e-5	5.3825e-4	9.8459e-1	9.9922e-1	9.9432e-1
	4	15	1.1270e-3	2.7406e-5	1.1500e-5	9.8516e-1	9.9964e-1	9.9939e-1
	5	20	1.0278e-3	8.1352e-6	2.2608e-5	9.8295e-1	9.9979e-1	9.9982e-1

Table 4 ANN error validation for urchin morphology

Neurons	Cycles	RMSE	MAD	AARE
1	5th	0.05378	0.03636	0.99304
	10th	0.02812	0.02102	0.60277
	25th	0.03570	0.02483	0.68864
	35th	0.44013	0.20959	44.97119
5	5th	0.00859	0.00619	0.17449
	10th	0.00713	0.00463	0.13190
	25th	0.00610	0.00340	0.09555
10	35th	0.02635	0.00170	41.81721
	5th	0.00197	0.00146	0.04311
	10th	0.00231	0.00151	0.04547
	25th	0.00315	0.00177	0.05321
15	35th	0.06706	0.00845	41.85923
	5th	0.11859	0.00467	0.13718
	10th	0.01220	0.00496	0.14296
	25th	0.01840	0.00447	0.12936
20	35th	0.17302	0.03350	42.49837
	5th	0.00627	0.00313	0.09007
	10th	0.00577	0.00281	0.07988
	25th	0.02805	0.01999	0.67574
	35th	0.12815	0.01870	41.98946

Table 5 ANN error validation for flower morphology

Neurons	Cycles	RMSE	MAD	AARE
1	1st	0.95611	0.02271	0.68844
	10th	0.02792	0.02003	0.60043
	20th	0.07727	0.05414	1.49511
5	1st	0.90224	0.62517	15.66858
	10th	0.75497	0.14301	14.30361
	20th	1.20527	0.84140	19.71740
10	1st	0.00869	0.00186	0.06244
	10th	0.00524	0.00190	0.06001
	20th	0.02081	0.00632	0.20033
15	1st	0.00610	0.00158	0.05017
	10th	0.00346	0.00159	0.04768
	20th	0.01539	0.00487	0.14260
20	1st	0.00444	0.00118	0.03737
	10th	0.00294	0.00148	0.04449
	20th	0.01297	0.00404	0.11282

RMSE jumps to 0.0263, and AARE increases dramatically to 41.82%, similar to the 1 neuron case. This suggests that despite the model's initial ability to predict behavior, complex processes such as capacity fading or parasitic reactions become dominant at longer cycles, which the 5 neuron model struggles to capture. With **10 neurons** the model showed excellent performance in early cycles (5th cycle

RMSE = 0.0019, AARE = 0.043%) exhibiting higher value of the R^2 ($R^2 = 0.99$). This suggests that it is very well suited for capturing the nuances introduced by the urchin morphology in the early-to-mid stages of cycling. However, by the 35th cycle, the model faces similar challenges as seen with fewer neurons, with RMSE increasing to 0.0671 and AARE jumping to 41.86%. This suggests that the battery's

electrochemical processes become highly unpredictable at longer cycling, and even this model configuration cannot account for those complex changes. Changing the configuration to **15 neurons** depicted that the model performs reasonably well in early cycles, its initial errors are higher than the 10-neuron model (5th cycle RMSE = 0.1186), indicating possible overfitting to early cycle data or noise. By the 35th cycle, the RMSE and AARE values spike (RMSE = 0.1730, AARE = 42.50%), indicating that the model fails to generalize and capture the complexity of the long-term behavior of the urchin morphology MnO_2 cathode. Similarly to the 10 and 15 neuron models the **20 neuron** configuration starts well, with low errors in the 5th and 10th cycles (e.g., RMSE = 0.0063 in the 5th cycle). However, by the 25th cycle, the RMSE jumps to 0.0281, and in the 35th cycle, it increases further (RMSE = 0.1282, AARE = 41.99%). This suggests that increasing the number of neurons beyond 10 does not necessarily lead to better performance for long-term cycle predictions and may even cause overfitting in earlier cycles. Significant increase in error at the 35th cycle across all models indicates that long-term cycling introduces complexities that even more advanced models struggle to predict, possibly due to degradation mechanisms not captured in the initial training data.

For flower morphology as tabulated in Table 5, a simple model with **1 neuron** exhibits high errors in the 1st cycle suggesting the model fails to comprehend the complex electrochemical dynamics of the LAB. The flower MnO_2 cathode's morphology and interaction with lithium ions are most likely to introduce nonlinear patterns that the 1 neuron model is unable to predict accurately. The model still performs poorly by the next 10th and 20th cycles, thus it suggests that the system's complexity demands more refined models to work effectively. While **5 neurons** configuration performs better than 1 neuron, the increasing RMSE in the 20th cycle suggests the model starts overfitting to the training data, losing its ability to generalize well. This could reflect the highly variable nature of the battery's electrochemical performance over time. MnO_2 cathodes in LAB tend to suffer from issues like passivation or clogging due to side reactions, which may add to the complexity of the model, and struggle to capture with only 5 neurons. With the **10 neurons** model the RMSE dramatically decreases to 0.0087, with MAD and AARE showing significant improvement (0.0019 and 0.062). The RMSE continues to improve slightly for the 10th and 20th cycles (0.0052 and 0.0208), with MAD and AARE

values remaining low, indicating robust predictive performance. This proposes that the model is efficiently apprehending battery behavior With 15 neurons in 1st cycle RMSE is 0.0061, presenting only a marginal increase in error compared to the 10-neuron model, while the MAD and AARE values continue to indicate high accuracy. For the 10th cycle, the performance is like the 10-neuron model, maintaining low error metrics, but there is a slight increase in the 20th cycle RMSE (0.0154). With **20 neurons** the 1st cycle RMSE is at 0.0044, which is the lowest among all configurations, suggesting excellent initial prediction capability. The MAD and AARE are also the lowest (0.0012 and 0.0374). The 10th and 20th cycles maintain low RMSE values, though a slight increase is observed in the 20th cycle (0.0129). Overall, this model shows the best performance, but the differences compared to the 10 neurons model are marginal. LAB involves intricate reaction mechanisms (OER), especially with a high surface area MnO_2 cathode. The low RMSE, MAD, and AARE suggest that this model configuration accurately predicts performance across the cycles without overfitting, indicating it can handle the complexities of the battery's behavior under various operating conditions. Both morphologies demonstrate similarities to the **10 neurons** model. This may suggest that the battery's behavior, while complex, does not require additional neurons beyond 10 for effective prediction. And graphical representation of best-selected neurons (10) is shown in Figs. 4 and 5 for both morphologies. The figures depicts the least error among both morphologies at 10 neurons. A important section of the study was the evaluation of the ANN model using an independent dataset, which allowed a more rigorous test of the model's generalization abilities. The performance of the model was evaluated by using three main metrics: RMSE, MAD, and AARE, for various training cycles. The predictive results of the model are tabulated in Table 6. The ANN model demonstrated strong performance in predicting battery characteristics at lower cycle counts (5, 15, and 25 cycles), with relatively low RMSE, MAD, and AARE values for MnO_2 with urchin morphology. This indicates that the model was able to generalize well to the independent dataset in these initial cycles.

However, as the cycle count increased to 35, a dramatic rise in RMSE, MAD, and AARE values was observed. This suggests that the model suffered from overfitting, due to degradation of battery performance as it can also be clearly seen in the experimental data in Fig. 1 that battery

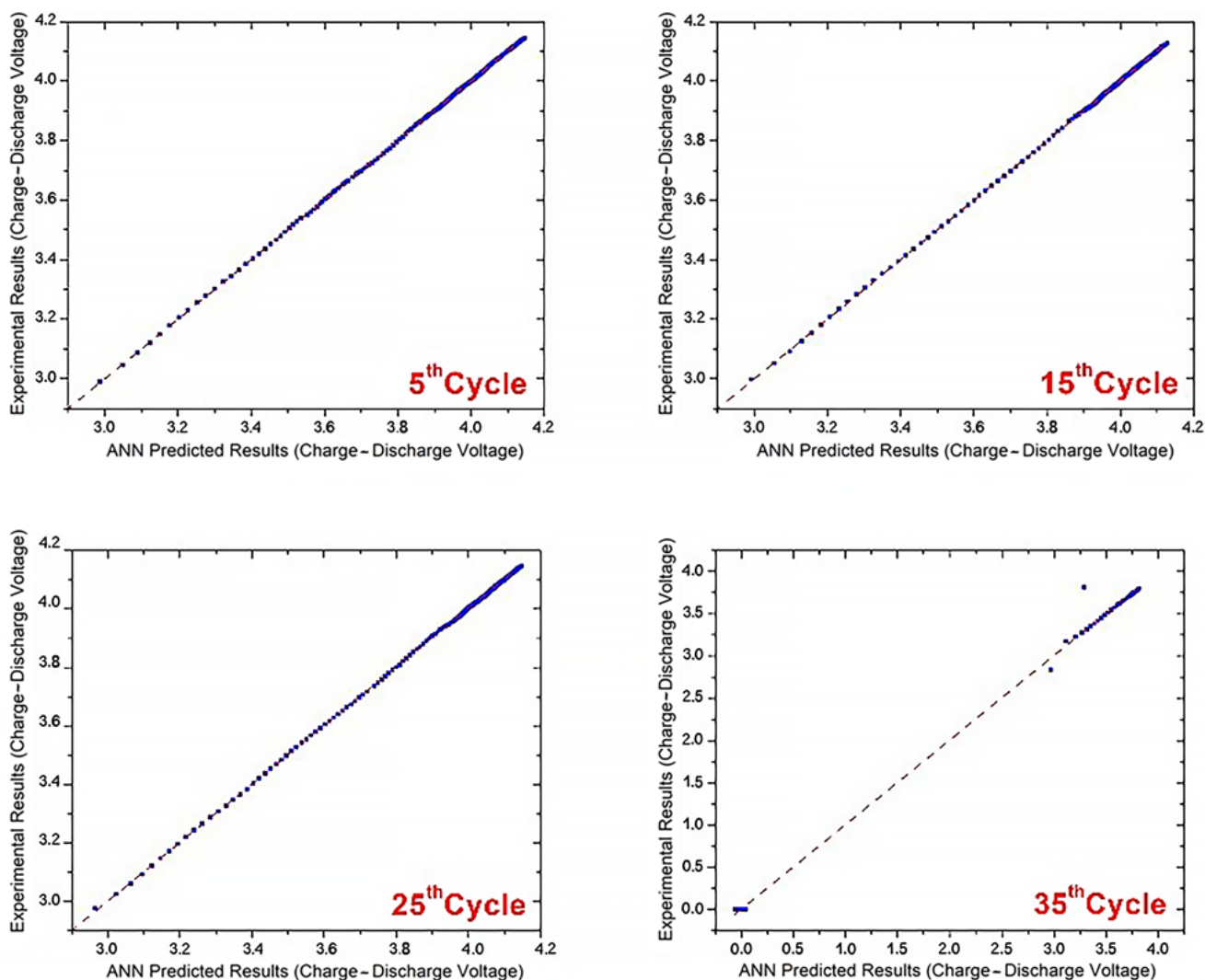


Fig. 4 Urchin-comparison of experimental results with ANN prediction (10 neurons model) for 5th, 15th, 25th and 35th cycles

stops before reaching the end conditions, where it became excessively tailored to the training data, causing a significant decline in its ability to predict accurately on unseen data. For the MnO_2 with flower morphology, the model performed reasonably well in the early cycles (1 and 10), with moderate RMSE and AARE values, indicating accurate predictions on the independent dataset. The MAD values also supported the model's generalization ability during these cycles. However, a sharp deterioration in performance was noted by cycle 20, as can be seen in Fig. 2, with noteworthy rises in RMSE, MAD, and AARE. Therefore, these models can be considered Robust for the prediction of charge/discharge voltage for LAB.

4 Implications of the study

The study suggests that extending the model by incorporating additional variables (temperature, current,

electrolyte composition) improves the predictive accuracy and dynamic control of LABs. However, the approach may not generalize to other battery chemistry without additional training and evaluation due to differences in reactions and degradation pathways. Overfitting observed during training highlights the importance of techniques like early stopping, cross validation and regularization. To scale the model for real world applications, expanding input features and datasets is essential to capture diverse operational conditions and complex LAB behavior.

5 Conclusions

This study employs ANN modelling to analyzed the charge/discharge voltage of LAB with two distinct MnO_2 morphologies ($\alpha\text{-MnO}_2$ and $\delta\text{-MnO}_2$).

While ANN has been extensively applied to LIBs. LABs present unique non-linear behavior and electrochemical

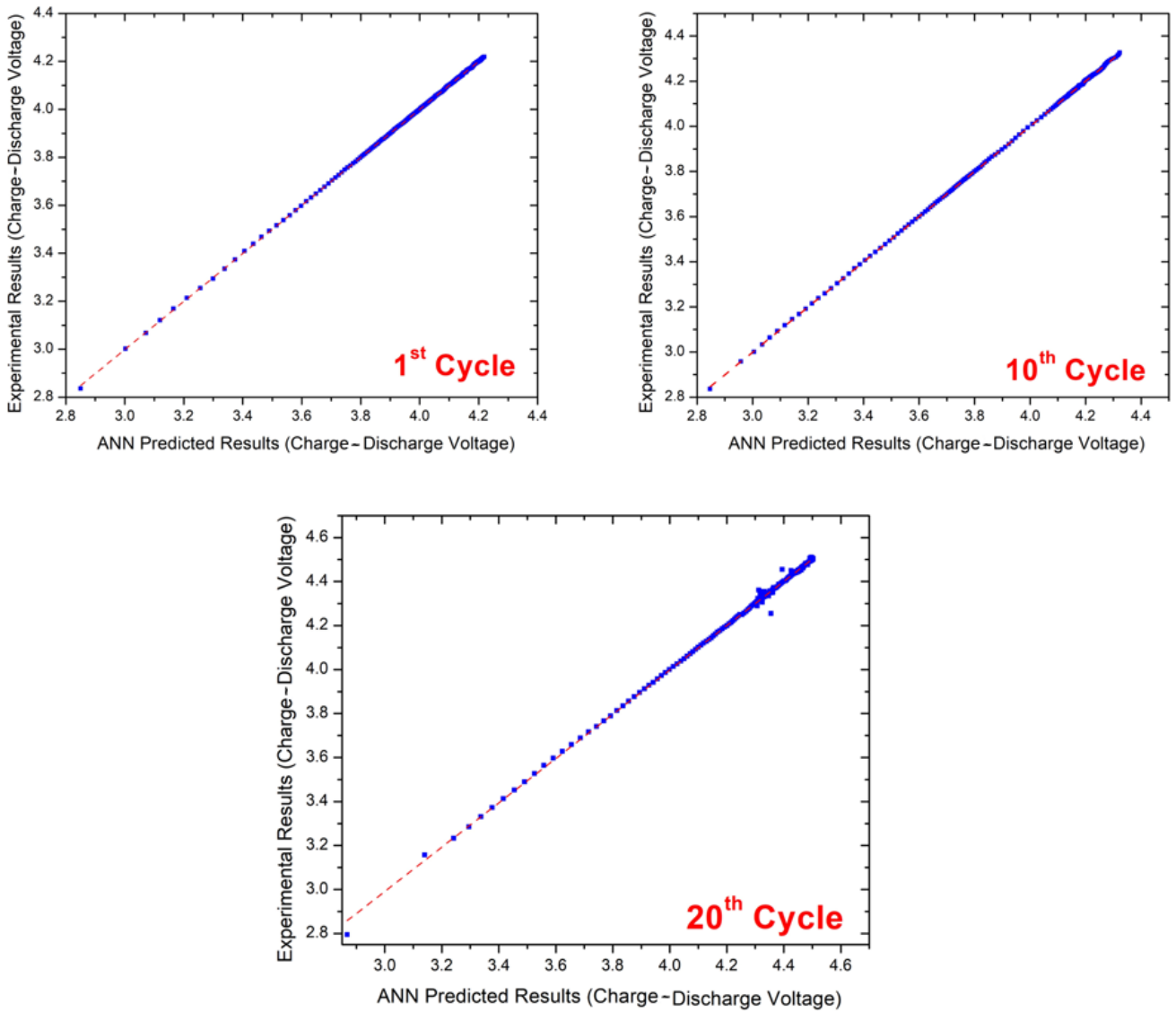


Fig. 5 Flower-comparison of experimental results with ANN prediction (10 neurons model) for 1st, 10th, and 20th cycle

Table 6 ANN errors validation for independent test data

Morphology	Cycles	RMSE	MAD	AARE
Urchins	5	0.00197	0.00155	0.04311
	15	0.00204	0.00141	0.05547
	25	0.00315	0.00167	0.05331
	35	0.05705	0.00844	40.95922
Flowers	1	0.00859	0.00185	0.06244
	10	0.00522	0.00209	0.06025
	20	0.02161	0.00532	0.18061

challenges, making ANN applications in this area largely unexplored. This research addresses this gap by developing a FFNN tailored to LABs with LM optimization enhancing model performance. The ANN predicts LAB voltages based on specific capacity, with neurons counts (1, 5, 10, 15 and 20) evaluated. A 10 neuron models proved optimal for

morphologies, balancing accuracy and complexity while achieving excellent predictive performance ($R^2 = 0.9998$). The results closely match the experimental data, with minimal MAD, RMSE and AARE errors, demonstrating ANN's ability to simulate complex electrochemical reactions. This study provides a foundation for further ANN applications in LABs, suggesting their potential for advancing predictive modelling in battery research and optimizing LAB performance.

Acknowledgement

The authors would like to acknowledged NED University of Engineering and Technology through ASRB grant number Acad/50(48)4394 and Ministry of Science and Technology under grant Acad/50(48)539 for providing financial assistance to conduct this research.

References

- [1] Li, F., Zhang, T., Zhou, H. "Challenges of non-aqueous Li-O₂ batteries: electrolytes, catalysts, and anodes", *Energy and Environmental Science*, 6(4), pp. 1125–1141, 2013.
<https://doi.org/10.1039/c3ee00053b>
- [2] Dunn, B., Kamath, Tarascon, J.-M. "Electrical energy storage for the grid: A battery of choices", *Science*, 334(6058), pp. 928–935, 2011.
<https://doi.org/10.1126/science.1212741>
- [3] Kraysberg, A. Ein-Eli, Y. "Review on Li-air batteries-opportunities, limitations and perspective", *Journal of Power Sources*, 196(3), pp. 886–893, 2011.
<https://doi.org/10.1016/j.jpowsour.2010.09.031>
- [4] Bruce, P. G. "Energy storage beyond the horizon: Rechargeable lithium batteries", *Solid State Ionics*, 179(21–26), pp. 752–760, 2008.
<https://doi.org/10.1016/j.ssi.2008.01.095>
- [5] Armand, M., Tarascon, J.-M. "Building better batteries", *Nature*, 451, pp. 652–657, 2008.
<https://doi.org/10.1038/451652a>
- [6] Ma, Z., Yuan, X., Li, L., Ma, Z.-F., Wilkinson, D. P., Zhang, L., Zhang, J. "A review of cathode materials and structures for rechargeable lithium-air batteries", *Energy and Environmental Science*, 8(8), pp. 2144–2198, 2015.
<https://doi.org/10.1039/C5EE00838G>
- [7] Ghouri, Z. K., Zahoor, A., Barakat, N. A. M., Alsoufi, M. S., Bawazeer, T. M., Mohamed, A. F., Kim, H. Y. "The (2 × 2) tunnels structured manganese dioxide nanorods with α phase for lithium air batteries", *Superlattices and Microstructures*, 90, pp. 184–190, 2016.
<https://doi.org/10.1016/j.spmi.2015.12.012>
- [8] Dawadi, S., Gupta, A., Khatri, M., Budhathoki, B., Lamichhane, G., Parajuli, N. "Manganese dioxide nanoparticles: synthesis, application and challenges", *Bulletin of Materials Science*, 43(2777), pp. 1–10, 2020.
<https://doi.org/10.1007/s12034-020-02247-8>
- [9] Awan, Z., Ghouri, Z. K., Hashmi, S. "Influence of Ag nanoparticles on state of the art MnO₂ nanorods performance as an electrocatalyst for lithium air batteries", *International Journal of Hydrogen Energy*, 43(5), pp. 2930–2942, 2018.
<https://doi.org/10.1016/j.ijhydene.2017.12.083>
- [10] Truong, T. T., Liu, Y., Ren, Y., Trahey, L., Sun, Y. "Morphological and crystalline evolution of nanostructured MnO₂ and its application in lithium-air batteries", *ACS Nano*, 6(9), pp. 8067–8077, 2012.
<https://doi.org/10.1021/nn302654p>
- [11] Ge, M.-F., Liu, Y., Jiang, X., Liu, J. "A review on state of health estimations and remaining useful life prognostics of lithium-ion batteries", *Measurement*, 174, 109057, 2021.
<https://doi.org/10.1016/j.measurement.2021.109057>
- [12] Qin, P., Zhao, L., Liu, Z. "State of health prediction for lithium-ion battery using a gradient boosting-based data-driven method", *Journal of Energy Storage*, 47, 103644, 2022.
<https://doi.org/10.1016/j.est.2021.103644>
- [13] Beltran, H., Sansano, E., Pecht, M. "Machine learning techniques suitability to estimate the retained capacity in lithium-ion batteries from partial charge/discharge curves", *Journal of Energy Storage*, 59, 106346, 2023.
<https://doi.org/10.1016/j.est.2022.106346>
- [14] Jain, A. K., Mao, J., Mohiuddin, K. M. "Artificial neural networks: A tutorial", *Computer*, 29(3), pp. 31–44, 1996.
<https://doi.org/10.1109/2.485891>
- [15] Boujouadar, Y., Elmoussaoui, H., Lamhamdi, T. "Lithium-ion batteries modeling and state of charge estimation using artificial neural network", *International Journal of Electrical and Computer Engineering*, 9(5), pp. 3415–3422, 2019.
<https://doi.org/10.11591/ijece.v9i5.pp3415-3422>
- [16] Jantharamin, N. "Battery modeling based on artificial neural network for battery control and management", In 2018 21st International Conference on Electrical Machines and Systems (ICEMS), Jeju, South Korea, 2018, pp. 2111–2114. ISBN 978-89-86510-20-1
<https://doi.org/10.23919/ICEMS.2018.8549015>
- [17] Zhang, G., Xia, B., Wang, J., Ye, B., Chen, Y., Yu, Z., Li, Y. "Intelligent state of charge estimation of battery pack based on particle swarm optimization algorithm improved radical basis function neural network", *Journal of Energy Storage*, 50, 104211, 2022.
<https://doi.org/10.1016/j.est.2022.104211>
- [18] Song, X., Yang, F., Wang, D., Tsui, K.-L. "Combined CNN-LSTM network for state-of-charge estimation of lithium-ion batteries", *IEEE Access*, 7, pp. 88894–88902, 2019.
<https://doi.org/10.1109/ACCESS.2019.2926517>
- [19] Soylu, E., Soylu, T., Bayir, R. "Design and implementation of SOC prediction for a li-ion battery pack in an electric car with an embedded system", *Entropy*, 19(4), 146, 2017.
<https://doi.org/10.3390/e19040146>
- [20] Zahoor, A., Jang, H. S., Jeong, J. S., Christy, M., Hwang, Y. J., Nahm, K. S. "A comparative study of nanostructured α and δ MnO₂ for lithium oxygen battery application", *RSC Advances*, 4(18), pp. 8973–8977, 2014
<https://doi.org/10.1039/C3RA47659F>
- [21] Zamaniyan, A., Joda, F., Behroozsarand, A., Ebrahimi, H. "Application of artificial neural networks (ANN) for modeling of industrial hydrogen plant", *International Journal of Hydrogen Energy*, 38(15), pp. 6289–6297, 2013.
<https://doi.org/10.1016/j.ijhydene.2013.02.136>
- [22] MathWorks "MATLAB, (Version R2017a)", [computer program] Available at: <https://www.mathworks.com/products/matlab.html> [Accessed: 06 February 2025]